Optics Communications 466 (2020) 125661

Contents lists available at ScienceDirect

Optics Communications

journal homepage: www.elsevier.com/locate/optcom

Correction performance estimation of atmospheric turbulence based on eigenmode method

Chengbin Jin [a,b], Xingyun Zhang [a], Wenqiang Sun [a,b], Nan Li [a,b], Quanquan Mu [a], Zhaoliang Cao [c,*], Yukun Wang [a,*], Li Xuan [a]

[a] State Key Laboratory of Applied Optics, Changchun Institute of Optics, Fine Mechanics and Physics, Chinese Academy of Science, 130033 Changchun, Jilin, China
[b] University of Chinese Academy of Science, Beijing 100049, China
[c] School of Mathematics and Physics, Suzhou University of Science and Technology, Suzhou, Jiangsu 215009, China

ARTICLE INFO

Keywords:
Adaptive optics
Eigenmode
Atmospheric turbulence
Partial correction

ABSTRACT

An eigenmode method is proposed to estimate the correction performance of atmospheric turbulence based on a deformable mirror (DM). On the basis of the eigenmode, a formula that describes the relationship among residual error, eigenmode N, and turbulence strength D/r_0 (D, telescope aperture, r_0, atmospheric coherence length) is derived. The eigenmode and the Zernike polynomial methods are compared, too. An experiment is conducted, and results validate the theoretical equations. Hence, the correction performance of atmospheric turbulence may be estimated with the eigenmode method. This result is helpful for conveniently designing and evaluating the adaptive optics system used for turbulence correction.

1. Introduction

Atmospheric turbulence strongly affects the image quality of ground-based large aperture telescopes [1,2] and the communication performance of the free space laser communications [3,4]. Adaptive optics systems (AOSs) have been widely used to overcome the effect of atmospheric turbulence by correcting the aberrations in time [5–9]. Normally, the correction performance of the AOS is estimated with Noll's method [10]:

$$\Delta_J = 0.5426 \cdot J^{-\frac{\sqrt{3}}{4}} \cdot (\frac{D}{r_0})^{5/6}, (J > 10), \quad (1)$$

here J is the first modes of Zernike polynomial, ΔJ is the residual error with partial correction, D is the telescope aperture, and r_0 is the atmospheric turbulence length respectively. With this equation, one can estimate how many Zernike modes need to selected for an AOS. However, while a deformable mirror (DM) is used to correct the turbulence, it is hard to accurately generate the Zernike modes because of the limitation of its surface quality and actuator structure. Then, the correction performance will be decreased for the DM based AOS. To improve the correction accuracy, an eigenmode method is proposed recently. Biru Wang et al. demonstrated that the eigenmode is ideal for aberration correction [11]. Tao Cheng et al. adopted the eigenmode of DM to correct the aberrations in the woofer-tweeter AOS [12]. Xizheng Ke et al. also improved the performance of free space laser communication system based on the eigenmode of DM [13]. Bing Dong et al. used the eigenmode of DM to clean up the laser beam [14].

From above we can see, the eigenmode method is suitable for the DM to correct the atmospheric turbulence. However, the correction effect of atmospheric turbulence is estimated with Zernike modes according to Eq. (1). There is no formula to describe the relation between the atmospheric turbulence and the eigenmode of DM. Consequently, it is expected to establish an equation to estimate the correction performance of AOS with the eigenmode of DM and the correction accuracy will be improved greatly. In other words, with the established formulas, lower number of actuators is needed and then, the cost and complexity of AOS will be reduced because of the improvement of the correction accuracy. Therefore, in this study, we propose a method to derive a formula for residual aberration as a function of eigenmode of DM and the turbulence strength. The Zernike mode and the eigenmode are then compared. Finally, an experiment is conducted to validate the formula.

2. Eigenmode of DM

2.1. Decomposition of aberration with eigenmode

The eigenmode of DM is a set of orthogonal bases derived from the influence function of DM. This eigenmode has the following characteristics. (a) the number of eigenmode is equivalent to that of the actuators of DM, (b) the eigenmodes are mutually orthogonal, and (c) the spatial frequency is arranged from low to high, corresponding to the number of eigenmodes N. The eigenmode may be constructed

* Corresponding authors.
E-mail addresses: caozl@usts.edu.cn (Z. Cao), wangyukun@ciomp.ac.cn (Y. Wang).

https://doi.org/10.1016/j.optcom.2020.125661
Received 25 December 2019; Received in revised form 21 February 2020; Accepted 1 March 2020
Available online 3 March 2020

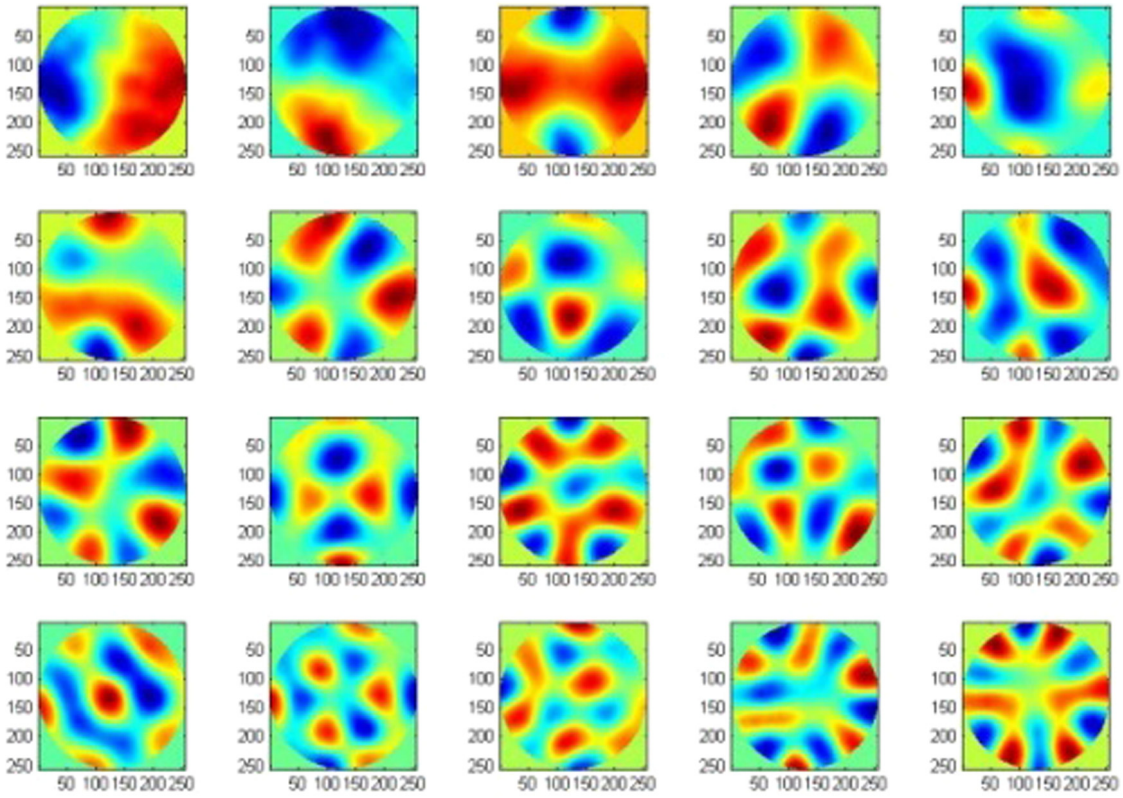

Fig. 1. Measured first 20 eigenmodes of DM.

with the influence function R of DM, which can be measured by a Shack–Hartmann wavefront sensor (S-H WFS) [15–17]. The wavefront produced by the DM can be represented by a linear combination of the influence function:

$$\Phi = \sum_i V_i \cdot R_i, \tag{2}$$

where R_i and V_i are the influence function and control voltage of the ith actuator, respectively. To describe the correlations of the influence functions of different actuators with orthogonal mode, a matrix C is defined as [18–20]:

$$C(i,j) = C(j,i) = D^{-1} \int_D R_i R_j dx dy, \tag{3}$$

here D is the aperture of DM. The matrix C may be decomposed with the singular value decomposition method:

$$C = USU^T, \tag{4}$$

where S is a diagonal matrix whose diagonal elements are the eigenvalue of matrix C, and U is a unitary matrix consisting of the eigenvector of C. The eigenmode matrix of DM may be expressed as:

$$\mathrm{M} = \mathrm{R} \cdot \mathrm{U}, \tag{5}$$

A random wavefront may be described by the eigenmode:

$$\Phi = \sum_i M_i m_i, \tag{6}$$

where m_i is the ith coefficient of M_i. Therefore, it can be decomposed by the eigenmodes for a random distorted wavefront detected by S-H WFS:

$$g = M \cdot m, \tag{7}$$

and the coefficients may be achieved as follows:

$$m = g \cdot M^{-1}, \tag{8}$$

where g is the measured distorted wavefront, and M^{-1} is the pseudo-inverse of the eigenmode matrix M. Given the known eigenmode matrix and the measured wavefront, the coefficients matrix can be calculated using Eq. (8).

To reconstruct the correction voltage signal with eigenmode, Eq. (7) may be rewritten as follows:

$$g = M \cdot m = R \cdot V, \tag{9}$$

where V is the voltage signal matrix, which must be solved. Combining Eqs. (5) and (9), we can obtain the following:

$$m = U^{-1} \cdot V, \tag{10}$$

The voltage can be eventually calculated as follows:

$$V = U \cdot m = U \cdot M^{-1} \cdot g, \tag{11}$$

The correction voltage signal may be computed using Eq. (11) with the eigenmode matrix and the measured distorted wavefront.

2.2. Measurement of eigenmode matrix of DM

A continuous surface DM (ALPAO, DM145-25) is selected with 145 actuators and an aperture of 25 mm to measure the eigenmode matrix. First, influence function R is measured by applying the unit voltage on each actuator individually. The phase response measured by a ZYGO interferometer is also recorded. The eigenmode matrix may be acquired according to Eqs. (3)–(5) with the measured influence function R. The patterns of the first 20 eigenmodes are shown Fig. 1. The spatial frequency of the wavefront is increased accordingly, which is similar to that of Zernike polynomials, with the increased number of modes. Consequently, the aberrations may be corrected by using the eigenmode of DM.

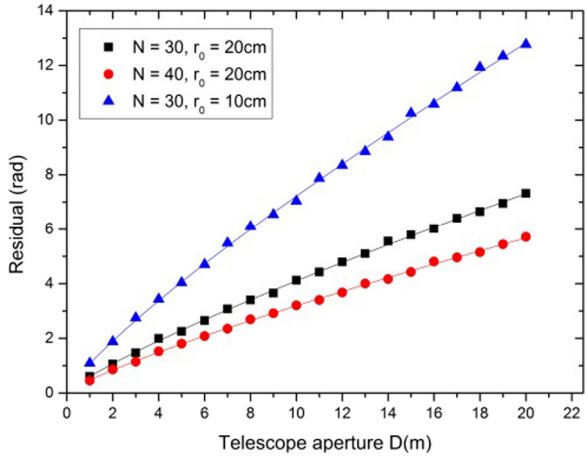

Fig. 2. Residual error as a function of telescope aperture.

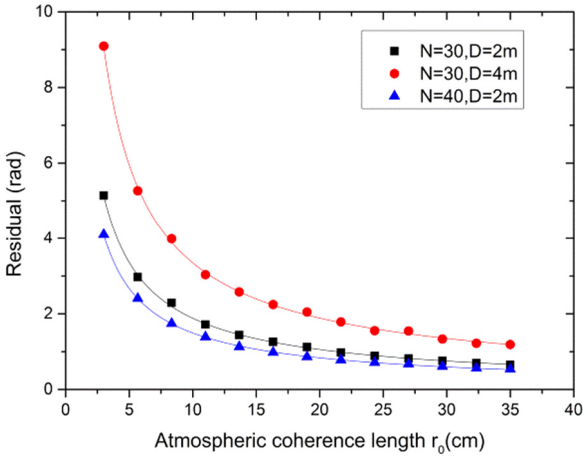

Fig. 3. Residual error as a function of r_0.

3. Correction performance analysis of atmospheric turbulence

3.1. Telescope aperture

Similar to the partial correction of turbulence with Zernike polynomials [21], the degree of correction of eigenmode is related to eigenmode N, telescope aperture D, and atmospheric coherence length r_0. The effect of D is considered first to obtain the residual error as a function of N, D, and r_0. The atmospheric turbulence is produced according to Kolmogorov's theory. A total of 100 random atmospheric turbulence wavefronts are generated with 404 Zernike modes to obtain a statistical average result. Assuming that the first N eigenmodes are used to correct the atmospheric turbulence, the residual wavefront may be calculated by the following:

$$\Phi_{res} = \Phi_{atmos} - \Phi_N, \tag{12}$$

where Φ_{atmos} is the random atmospheric turbulence wavefront, and Φ_N represents the fitted wavefront with the first N eigenmode. The statistic average root mean square (RMS) value of Φ_{res} is computed as the residual error because the turbulence is random. The relationship between telescope aperture D and the residual wavefront is calculated, as illustrated in Fig. 2 with different N and r_0. The dots are the computed data, and the real lines are the fitted curves. Given that N and r_0 are fixed, the residual error may be fitted with the following:

$$\Phi_{res} = a(N, r_0) \cdot D^{5/6}, \tag{13}$$

where $a(N, r_0)$ is a coefficient related to N and r_0. All calculated data are perfectly fitted with Eq. (13). Although only three curves are shown in Fig. 2, much computed data are fitted well. Hence, the residual wavefront is proportional to the 5/6 power of D.

3.2. Atmospheric coherence length

The relationship between the residual error and atmospheric coherence length r_0 is also calculated, as demonstrated in Fig. 3 with the condition of $N = 30$ and $D = 2$ m, $N = 40$ and $D = 2$ m, and $N = 30$ and $D = 4$ m. According to Eq. (13), the residual error may be fitted by the following equation:

$$\Phi_{res} = b(N) \cdot (\frac{D}{r_0})^{5/6}, \tag{14}$$

where $b(N)$ is a coefficient related with eigenmode N. The computed data are fitted fine with Eq. (14). Therefore, the residual wavefront error is inverse proportional to the 5/6 power of r_0 and proportional to the 5/6 power of D/r_0. The turbulence strength may be described by the D/r_0: larger the D/r_0 is, the stronger the turbulence. Thus, the residual error becomes large after the adaptive correction for strong turbulence.

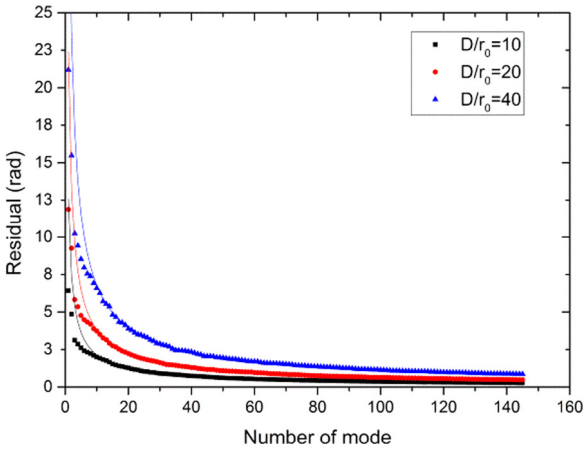

Fig. 4. Residual error as a function of eigenmode N.

3.3. Eigenmode of DM

The residual error is computed with different N at the condition of $D/r_0 = 10$, 20, and 40. The following formula is used to fit the data:

$$\Phi_{res} = c \cdot N^{\alpha} \cdot (\frac{D}{r_0})^{5/6}, \tag{15}$$

However, the fitting results show that α and c are not constant, and the fitting error is large. Considering Noll's formula with limit of the Zernike modes larger than 10, we also utilize $N > 10$ to fit the calculated data, and the fitted results are shown in Fig. 4. When $N > 10$, the discrete data are fitted well with $c = 1.846$ and $\alpha = -4\sqrt{3}/9$. Consequently, the residual error can be expressed as ($N > 10$):

$$\Phi_{res} = 1.846 \cdot N^{-\frac{4\sqrt{3}}{9}} \cdot (\frac{D}{r_0})^{5/6}, \tag{16}$$

where the units of D and r_0 are meter, and the unit of the RMS error of Φ_{res} is rad.

When $N \leq 10$, the computed data are fitted for each eigenmode separately, and the results are shown in Table 1. With Eq. (16) and formulas in Table 1, the residual error may be calculated at different N, D, and r_0. Thus, the correction performance of the atmospheric turbulence may be estimated based on the eigenmode. Fig. 5 illustrates the residual error as functions of N and D/r_0. The residual error may be easily evaluated with the eigenmode of DM. For example, for a telescope with $D = 2$ m and $r_0 = 10$ cm, the first 57 eigenmodes should be used to correct the atmospheric turbulence with the condition that the residual error is 1 rad.

Table 1
First 10 formulas of RMS.

$\Phi_{N=1} = 0.958 \cdot (\frac{D}{r_0})^{5/6}$	$\Phi_{N=6} = 0.367 \cdot (\frac{D}{r_0})^{5/6}$
$\Phi_{N=2} = 0.735 \cdot (\frac{D}{r_0})^{5/6}$	$\Phi_{N=7} = 0.344 \cdot (\frac{D}{r_0})^{5/6}$
$\Phi_{N=3} = 0.476 \cdot (\frac{D}{r_0})^{5/6}$	$\Phi_{N=8} = 0.337 \cdot (\frac{D}{r_0})^{5/6}$
$\Phi_{N=4} = 0.437 \cdot (\frac{D}{r_0})^{5/6}$	$\Phi_{N=9} = 0.317 \cdot (\frac{D}{r_0})^{5/6}$
$\Phi_{N=5} = 0.385 \cdot (\frac{D}{r_0})^{5/6}$	$\Phi_{N=10} = 0.301 \cdot (\frac{D}{r_0})^{5/6}$

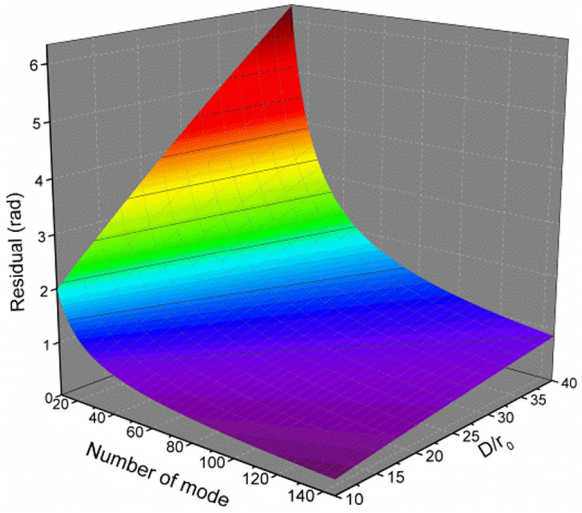

Fig. 5. Residual error as functions of eigenmode N and D/r_0.

3.4. Comparison

The Zernike polynomials and the eigenmode method are performed. According to Noll's work, when the first J Zernike modes are corrected, the RMS value of the residual wavefront can be calculated with Eq. (1). For comparison, the residual error is computed with the same number of modes under the condition of $D/r_0 = 20$, as shown in Fig. 6. The residual error of eigenmode is larger than that of Zernike mode when the number of modes is lower than 38. Moreover, the residual error of Zernike mode is larger when the number of modes is larger than 38.

The improvement ratio of eigenmode is defined as follows to evaluate the overall correction error compared with the Zernike mode.

$$R_{eigen} = \frac{\Delta_J - \Phi_{res}}{\Delta_J} = 1 - \frac{\Phi_{res}}{\Delta_J}, \tag{17}$$

Substituting Eqs. (1) and (16) into Eq. (17), R_{eigen} can be rewritten as follows:

$$R_{eigen} = 1 - \frac{17}{5} \cdot N^{\frac{-7\sqrt{3}}{36}}, \tag{18}$$

As we can see, R_{eigen} has no relationship with turbulence strength D/r_0 but is only related to the number of modes. The R_{eigen}, as a function of N, is calculated, as shown in Fig. 7. It illustrates that R_{eigen} is nonlinearly increased as the number of modes increased. For example, compared with the Zernike mode, the residual error is reduced by approximately 36% when the number of modes is 145. Hence, the eigenmode method can be used to improve the correction accuracy when the number of modes is larger than 38 for different turbulence strengths.

4. Experiment validation

An experimental AOS is established to verify the proposed method and the optical layout is illustrated in Fig. 8. A 785 nm laser output

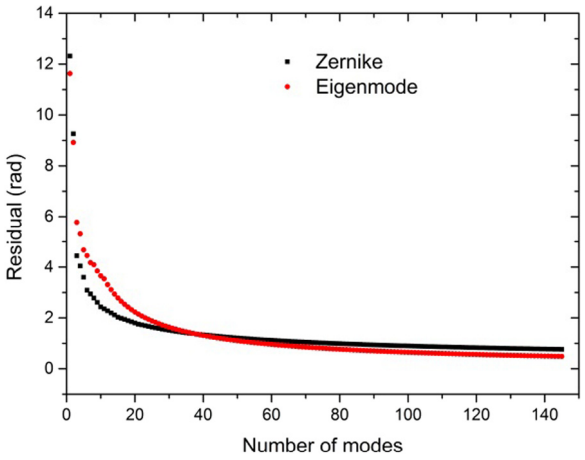

Fig. 6. Residual error of eigenmode and Zernike mode with $D/r_0 = 20$.

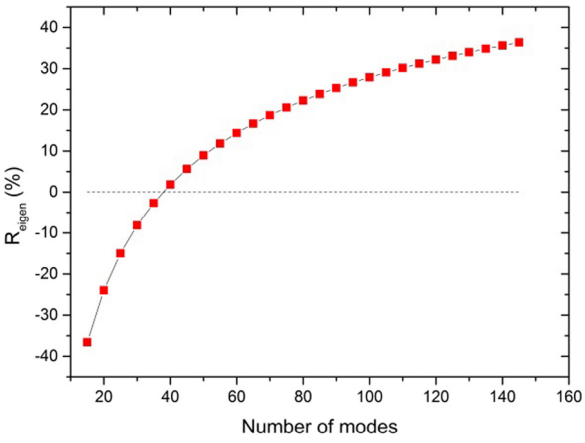

Fig. 7. Relationship between R_{eigen} and mode number N.

with the fiber is collimated by a lens and goes through an atmospheric turbulence simulator. The collimated light is reflected by a DM and zoomed in with a 4f lens system. The zoomed beam is split into two beams: one goes to an S-H WFS for wavefront detection; the other is focused on a CCD imaging camera. The DM is the same as what is used to measure the eigenmode. An S-H WFS with the frame rate of 2.7 kHz and 20 × 20 microlenses is selected to measure the wavefront. To perform the wavefront correction, the distorted wavefront is measured by the S-H WFS firstly; then, the control signal can be calculated with Eqs. (7), (8) and (11) according to the measured wavefront; at last, the control signal is sent to the DM and the distortions may be corrected. After correction, the corrected wavefront can be achieved with the S-H WFS and the clear image of the fiber bundle can be observed at the CCD camera. The atmospheric turbulence simulator (Lexitek) is selected to induce a random turbulence with the parameters of 100 mm aperture, and r_0 = 1 mm at the wavelength of 785 nm. The effective beam aperture (sub-aperture) is 20 mm, and the turbulence strength $D/r_0 = 20$. To satisfy the frozen flow hypothesis, a sub-aperture stop is placed at the edge of the turbulence simulator.

For comparison, a distorted wavefront is corrected with the eigenmode and Zernike methods. First, a static aberration is detected and corrected with the modes of 20, 40, and 50. The corrected results are shown in Figs. 9 and 10. Fig. 9 illustrates that the RMS of the distorted wavefront is 7.54 rad before correction (Fig. 9(a)); after the correction of the first 20, 40, and 50 modes, the RMS error of the distortion is reduced to 3.67, 1.88, and 1.17 rad for the eigenmode method, respectively, and 3.24, 1.98, and 1.45 rad for the Zernike polynomial

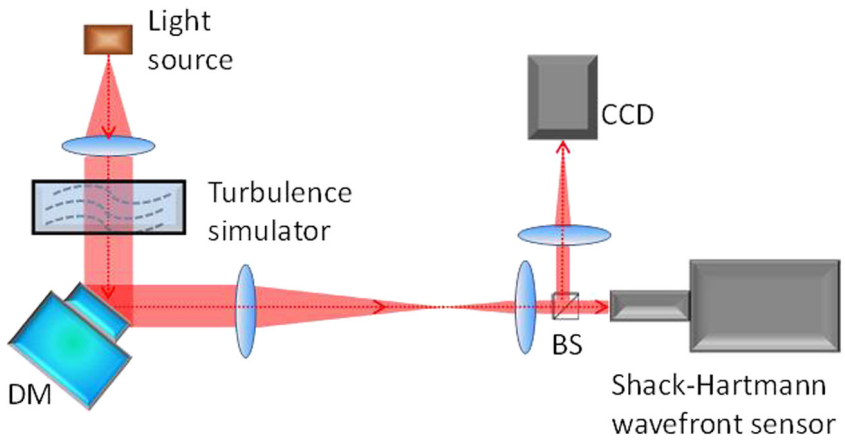

Fig. 8. Diagram of experiment AOS.

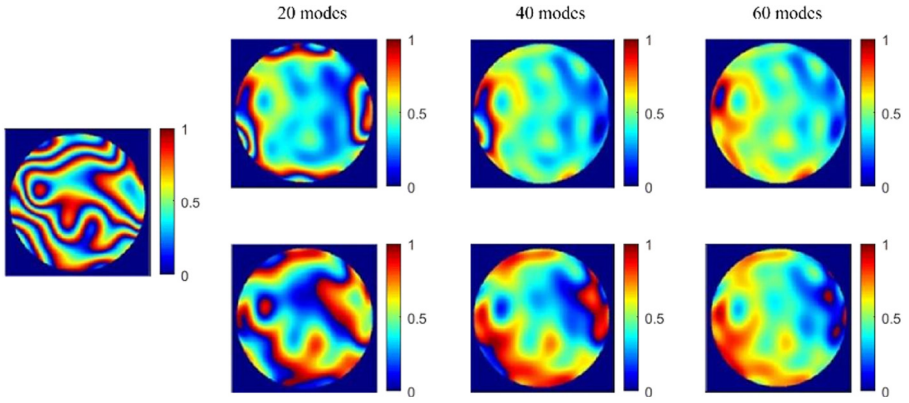

Fig. 9. Distorted wavefront: (a) before correction and (b) after correction with different modes: the upper is the corrected wavefront for the eigenmode, and the lower is that for the Zernike mode.

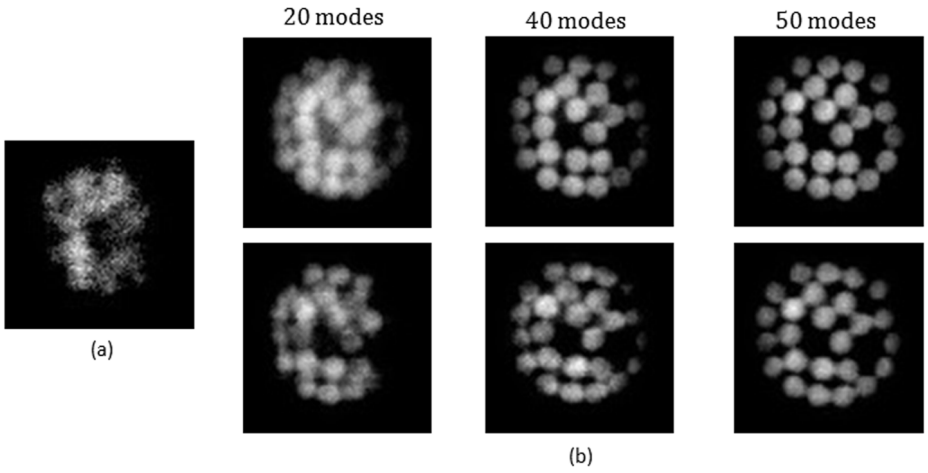

Fig. 10. Image of fiber bundle: (a) without correction and (b) after correction with different modes: the upper is the corrected wavefront for the eigenmode, and the lower is that for the Zernike mode.

method, respectively (Fig. 9(b)). The experimental results indicate that the residual error of eigenmode is larger than that of the Zernike method when the number of modes is less than 38, whereas the residual error of eigenmode is lower than that of Zernike mode. These results are similar to the calculated results in Figs. 6 and 7. Fig. 10 displays the imaging results of the fiber bundle before and after correction with the eigenmode and the Zernike method. The image of fiber bundle becomes clear as the corrected modes increase for the eigenmode and Zernike methods. Furthermore, the resolution of the fiber bundle image with the correction of 20 eigenmodes is lower than that with the correction of 20 Zernike modes. However, for the correction with 40, and 50 modes, the image resolution of eigenmode is higher than that of the Zernike mode. Therefore, the validity of Eq. (18) is verified.

The dynamic atmospheric turbulence is corrected to validate our proposed method. The turbulence simulator may be rotated with a motor to simulate the dynamic turbulence. To get a statistical average effect, twenty positions are selected with equal interval while the turbulence simulator rotates a round. At each position, the wavefront

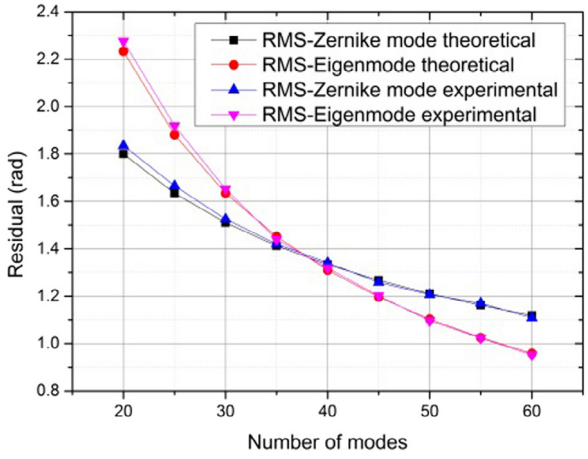

Fig. 11. Residual error as a function of the number of modes for eigenmode and Zernike methods.

is detected and corrected and the residual error is recorded. Then, the statistical average value can be calculated with the recorded results, and the statistical results are shown in Fig. 11. For comparison, the theoretical curves are also provided in Fig. 11. The experimental results are close to the theoretical curves for the eigenmode and Zernike methods. Moreover, the crosspoint of the experimental curves of eigenmode and Zernike methods approaches that of the theory. Consequently, all experimental results validate our proposed method and then, the established relation between the eigenmode and the atmospheric turbulence is valid.

5. Discussions and conclusions

An eigenmode method is used to estimate the correction performance of atmospheric turbulence. A total of 100 random atmospheric turbulence wavefronts are generated with 404 Zernike modes to simulate the atmospheric turbulence correction on the basis of the eigenmode. Residual wavefronts are calculated with the first N eigenmode used for turbulence correction. The residual error as functions of eigenmode N and turbulence strength D/r_0 is achieved with the fitting results of the computed data. The residual wavefront error is proportional to the 5/6 power of D/r_0 and the $-4\sqrt{3}/9$ power of N. The acquired formula may be used to determine how many eigenmodes are needed for an AOS used for large aperture telescope.

Finally, an experiment is performed to validate the established formulas. The experimental results are close to the theoretical curves, which illustrate that the equations are effective. Therefore, while using the eigenmode of DM to correct the turbulence, the correction performance can be estimated with the established formulas. Furthermore, the eigenmode and Zernike methods are compared with the theoretical and experimental results. The residual error of eigenmode is larger than that of Zernike mode when the number of modes is lower than 38, whereas the residual error of Zernike mode is larger than that of eigenmode.

Although a concrete DM with continuous face-sheet is utilized to produce the eigenmode matrix, generally, the response of the actuator is a Gauss pattern, and different continuous face-sheet DMs exhibit a similar response pattern. Hence, the proposed method is suitable for continuous face-sheet DMs. For the segmented and bimorph DMs, the proposed method is still effective to acquire the correction performance of atmospheric turbulence with the eigenmode of DM. but, the formulas are possibly different to those presented in this paper. Anyhow, the proposed method may be used to evaluate the correction ability of the DM when utilized to correct the atmospheric turbulence. Thus, an eigenmode method is established for estimation of the correction performance of the atmospheric turbulence on the basis of the DM. This work can help in designing the AOS and estimating the correction ability of the DM based on eigenmode.

Declaration of competing interest

The authors declare that they have no known competing financial interests or personal relationships that could have appeared to influence the work reported in this paper.

CRediT authorship contribution statement

Chengbin Jin: Conceptualization, Methodology, Investigation, Writing - original draft. **Xingyun Zhang:** Software. **Wenqiang Sun:** Visualization. **Nan Li:** Visualization. **Quanquan Mu:** Funding acquisition. **Zhaoliang Cao:** Methodology, Writing - review & editing. **Yukun Wang:** Methodology, Software. **Li Xuan:** Funding acquisition.

Acknowledgment

This work is supported by the National Natural Science Foundation of China with grant numbers 61805238 and 61811530061.

References

[1] V.I. Tatarskii, V.U. Zavorotny, Atmospheric turbulence and the resolution limits of large ground-based telescopes: comment, J. Opt. Soc. Amer. A 10 (1993) 2410–2414.
[2] Lidia A. Bolbasova, Vladimir P. Lukin, Modal phase correction for large-aperture ground-based telescope with multiguide stars, in: Optics in Atmospheric Propagation and Adaptive Systems XII, in: Proc. SPIE, vol. 7476, 2009, p. 74760M.
[3] Aniceto Belmonte, Joseph M. Kahn, Approaching fundamental limits to free-space communication through atmospheric turbulence, in: Broadband Access Communication Technologies XII, in: Proc. SPIE, vol. 10559, 2018, p. 105590E.
[4] A. Belmonte, J.M. Kahn, Satellite downlink coherent laser communications, in: M. Uysal, C. Capsoni, Z. Ghassemlooy, A. Boucouvalas, E. Udvary (Eds.), Optical Wireless Communications: An Emerging Technology, Springer International Publishing, Cham, 2016, pp. 325–343.
[5] G. Herriot, S. Morris, A. Anthony, D. Derdall, D. Duncan, J. Dunn, A. Ebbers, J.M. Fletcher, T. Hardy, B. Leckie, A. Mirza, C. Morbey, M. Pfleger, S. Roberts, P. Shott, M. Smith, L. Saddlemyer, J. Sebesta, K. Szeto, B. Wooff, W. Windels, J.P. Veran, Progress on altair: The gemini north adaptive optics system, in: Proc. SPIE 2000, 4007, pp. 115–125.
[6] G. Rousset, F. Lacombe, P. Puget, E. Gendron, R. Arsenault, P. Kern, D. Rabaud, P.Y. Madec, N. Hubin, G. Zins, E. Stadler, J. Charton, P. Gigan, P. Feautrier, Status of the VLT Nasmyth adaptive optics system (NAOS), in: Proc. SPIE 2000, 4007, pp. 72–81.
[7] H. Takami, S. Colley, M. Dinkins, M. Eldred, O. Guyon, T. Golota, M. Hattori, Y. Hayano, M. Ito, M. Iye, S. Oya, Y. Saito, M. Watanabe, Status of Subaru laser guide star AO system, in: Proc. SPIE 2006, 6272, 62720C.
[8] C.E. Max, B.A. Macintosh, S. Gibbard, D.T. Gavel, H.G. Roe, I. de Pater, A.M. Ghez, D.S. Acton, P.L. Wizinowich, O. Lai, Neptune and Titan observed with Keck telescope adaptive optics, in: Proc. SPIE 2000, 4007, pp. 213–220.
[9] J. Angel, Ground-based imaging of extrasolar planets using adaptive optics, Nature 368 (1994) 203–207.
[10] Robert J. Noll, Zernike polynomials and atmospheric turbulence, J. Opt. Soc. Amer. 66 (1976) 207–211.
[11] B. Wang, Martin J. Booth, Optimum deformable mirror modes for sensorless adaptive optics, Opt. Commun. 28 (2009) 4467–4474.
[12] T. Cheng, W. Liu, K. Yang, X. He, P. Yang, B. Xu, Projection-based decoupling algorithm for a woofer–tweeter adaptive optics system, Opt. Eng. 57 (6) (2018) 065101.
[13] X. Ke, M. Li, Laser beam distorted wavefront correction based on deformable mirror eigenmodes, Opt. Eng. 58 (12) (2019) 126101.
[14] Bing Dong, Rui Wang, Laser beam cleanup using improved model-based wavefront sensorless adaptive optics, Chin. Opt. Lett. 14 (2016) 031406–31409.
[15] M.B. Roopashree, A. Vyas, Influence function measurement of continuous membrane deformable mirror actuators using Shack Hartmann sensor, AIP Conf. Proc. 1391 (2011) 453–455.
[16] K. Wang, W. Sun, Christopher T. Richie, Brandon K. Harvey, Eric Betzig, N. Ji, Direct wavefront sensing for high-resolution in vivo imaging in scattering tissue, Nature Commun. 6 (2015) 7276.
[17] G.Y. Yoon, T. Jitsuno, M. Nakatsuka, S. Nakai, Shack Hartmann wave-front measurement with a large F-number plastic microlens array, Appl. Opt. 35 (1) (1996) 188–192.

[18] E. Li, Y. Dai, H. Wang, Y. Zhang, Application of eigenmode in the adaptive optics system based on a micromachined membrane deformable mirror, Appl. Opt. 45 (2006) 5651–5656.
[19] T. Cheng, W. Liu, K. Yang, X. He, P. Yang, B. Xu, Testing for a slope-based decoupling algorithm in a woofer-tweeter adaptive optics system, Appl. Opt. 57 (2018) 3357–3364.
[20] B. Dong, R. Wang, Laser beam clean up using improved model-based wavefront sensorless adaptive optics, Chin. Opt. Lett. 14 (3) (2016) 031406.
[21] F. Sun, Z. Cao, Y. Wang, C. Zhang, X. Zhang, Y. Liu, Q. Mu, L. Xuan, DM/LCWFC based adaptive optics system for large aperture telescopes imaging from visible to infrared waveband, Opt. Express 24 (2016) 27494–27508.